Sublimation of Higher Fullerenes and Their Interaction with Silicon (100) Surface

M. Moalem*

Department of Nuclear Engineering, University of California, Berkeley, California 94720

M. Balooch and A. V. Hamza

Chemistry and Material Science Division, Lawrence Livermore National Laboratory, Livermore, California 94550

R. S. Ruoff

Molecular Physics Laboratory, SRI International, Menlo Park, California 94025

Received: June 14, 1995[⊗]

The heat of sublimation of C_{60}, C_{70}, C_{78}, C_{84}, and C_{96} is measured by modulated molecular beam mass spectrometry (MMBMS). For a mixture of these fullerenes the heat of sublimation is 39 ± 5, 43 ± 5, 47 ± 18, 59 ± 6, and 65 ± 11 kcal/mol, respectively, and did not change with the variation in composition. The partial pressure of C_{84} is estimated to be $P_{84} = 7.0 \times 10^{12}$ exp[−59.4 kcal/mol/*RT*] Torr. The scattering of C_{70} and C_{84} from Si(100) is also investigated by MMBMS. The behavior of C_{84} is quite similar to that of C_{60} reported earlier By Hamza, Balooch, and Moalem (*Surf. Sci.* **1994**, *317*, L1129) except that the onset of surface decomposition of the fullerene occurs at 850 K, 150 K lower than for C_{60}. When the surface temperature reaches 1000 K, total decomposition of the incident C_{84} is observed. The behavior of C_{70} is surprisingly different from both C_{60} and C_{84}. Twenty percent of the incident C_{70} decomposes at 1000 K, and the remaining 80% does not decompose until a target temperature of 1200 K is reached. At surface temperatures below 800 K, for the interaction of C_{70} and C_{84} with silicon, the dominant surface processes are adsorption with near perfect sticking probability, followed by surface diffusion to the edge of the specimen and desorption. The ratio of desorption rate constant k_d, to diffusion coefficient, D_s, for C_{70} and C_{84} was calculated to be 2.7×10^{16} exp(−40 (kcal/mol/*RT*) and 7.8×10^7 exp(−22 (kcal/mol/*RT*) cm^{-2}, respectively.

Introduction

A large database of information is beginning to emerge about the physical and chemical properties of C_{60} and C_{70}. The heat of sublimation, vapor pressure,[2−4] and kinetics of interaction of C_{60} and C_{70} with various surfaces[1,5] have been reported. In contrast, less is known about the physical properties of the larger fullerenes such as C_{78}, C_{84}, and C_{96}. These higher fullerenes have unique structures and interesting potential applications.[6,7] C_{84} has two dominant isomers, D_2 and D_{2d}, which have only recently become the subject of study.[8,9] Obtaining pure, 0.1 g quantities of C_{76} and larger fullerene samples has been difficult because they are only minor products in the production of fullerene soot.

The adsorption of C_{84} on Si(100)-(2×1) has been investigated by scanning tunneling microscopy (STM).[10] The first monolayer of C_{84} bonds strongly to the surface and can never be desorbed by heating. C_{84} instead reacts with the silicon surface to form SiC at surface temperatures above 1000 °C. Multilayers of C_{84} desorb from the Si(100)-(2×1) substrate easily at approximately 400 °C. The multilayer exhibits an fcc structure.

Thin films of single-crystal C_{84} were grown on mica, and the lattice parameter was determined by transmission electron microscopy.[11] The films were lifted from the mica substrate with water. The structure was fcc and did not undergo a phase transition upon cooling to 160 K.

The electronic structures of C_{84} and C_{76} have been investigated by photoelectron spectroscopy and electron energy loss spectroscopy.[12−16] The valence orbitals are very similar to C_{60} except that the states are smeared out due to the symmetry break in the C_{76} and C_{84} structures.

We have used the Knudsen cell modulated molecular beam mass spectrometric technique to study the vaporization of fullerene mixtures and the scattering properties of the fullerenes C_{70} through C_{96} and have also investigated the interactions of C_{70} and C_{84} with the silicon (100) surface as a function of temperature. The scattering results are also compared to similar measurements made with C_{60}.[1,5]

Experiment

Three types of specimens were used for this investigation. Pure C_{60} and C_{70} were obtained from Texas Fullerenes Co. Large quantities of purified higher fullerenes (>C_{70}) were not commercially available, and therefore, a mixture rich in higher fullerenes was prepared. Fullerene soot containing a mixture of different fullerenes was obtained from MER Corp. The soot was first extracted with toluene, and the extract was dried; the resulting solid was then extracted to selectively enrich the mixture in larger fullerenes (i.e. C_{84}), washed with diethyl ether, and dried. Figure 1 shows the mass spectrum of fullerenes in this sample as obtained by surface analysis by laser-induced-desorption mass spectrometry (SALI). SALI utilizes a 10.6 eV single-photon ionization of neutral C_m desorbed from a surface: signal intensities approximately reflect the actual [C_m] present. By far, the largest peaks in the spectrum are those of C_{84} and C_{70}. C_{78} and C_{96} are also present at substantial levels, while C_{60} constitutes only 0.05% of the recorded counts.

The system is described in detail elsewhere.[5] Briefly, it consists of three differentially pumped vacuum chambers. The

* To whom correspondence should be addressed.

⊗ Abstract published in *Advance ACS Abstracts*, September 15, 1995.

0022-3654/95/2099-16736$09.00/0

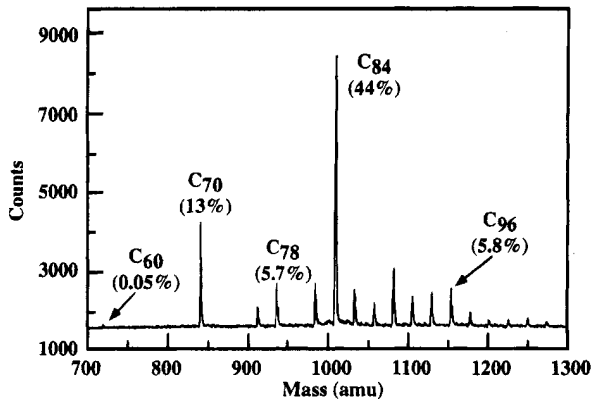

Figure 1. Surface analysis by laser-induced-desorption (SALI) time-of-flight mass spectrum of species contained in fullerene mixture specimens prepared. The desorption photon and ionization photon energy is 10.6 eV.

source chamber, pumped to a base pressure of $<6 \times 10^{-8}$ Torr by a diffusion pump, houses the molecular beam source. The solid specimen is held inside an annular Knudsen cell. The 1 mm source orifice of the Knudsen cell is laser aligned using quartz windows on the opposite end. A heater insulated by boron nitride encases the Knudsen cell. Temperatures (monitored by a K-type thermocouple) up to ~1300 K can be achieved. The gas molecules effuse out of the orifice and form a molecular beam. A rotating sawtooth disk intercepts the beam and produces a square-wave modulation. The modulation frequency is monitored by an optical switch made of a light source and photo diode between which the rotating disk passes. Before each new experiment, the source was vacuum annealed for 2 h at 400 °C to remove solvent residues.

A collimating orifice 1 mm in diameter separates the source and target chambers. The target chamber is pumped by a cryopump to $<1 \times 10^{-9}$ Torr. For measurements of ionization efficiency and heat of sublimation of fullerenes, the molecular beam is sampled directly by an in-line off-axis quadrupole mass spectrometer (QMS). The fullerenes are ionized by electron-impact ionization, extracted, and filtered by a quadrupole mass filter having mass detection up to 1400 amu. The output signal of the QMS is processed by a lock-in amplifier using the reference signal from the optical switch. This technique significantly reduces the background noise prevalent in non-modulated experiments.

For surface interaction studies, the beam is scattered from a silicon disk 6 mm in diameter at a 45° angle of incidence. The target is heated from behind by a buttom heater, and its temperature is measured by an infrared pyrometer. Before the experiment the sample is briefly heated to 1300 K to remove the native oxide. For scattering experiments with SiO_2, the silicon disk was preoxidized at 1100 K to a thickness of ~200 Å. The scattered beam from the target passes through a collimating orifice and enters the detector chamber. The detector chamber is pumped by an ion pump to a pressure $<3 \times 10^{-10}$ Torr and houses the second QMS. The scattered signal at high target temperatures is detected by the lock-in detection technique described above. At low temperature, modulation of the beam can yield detailed kinetic and mechanistic information of the gas–surface interaction. Unfortunately, even the simplest of systems have complicated interactions including for example surface diffusion; see ref 4. The analysis of the modulated signal will be published elsewhere. The unmodulated experiment is reported here for qualitative comparison. The chopper is turned off and the QMS signal is directly measured with an electrometer for this experiment.

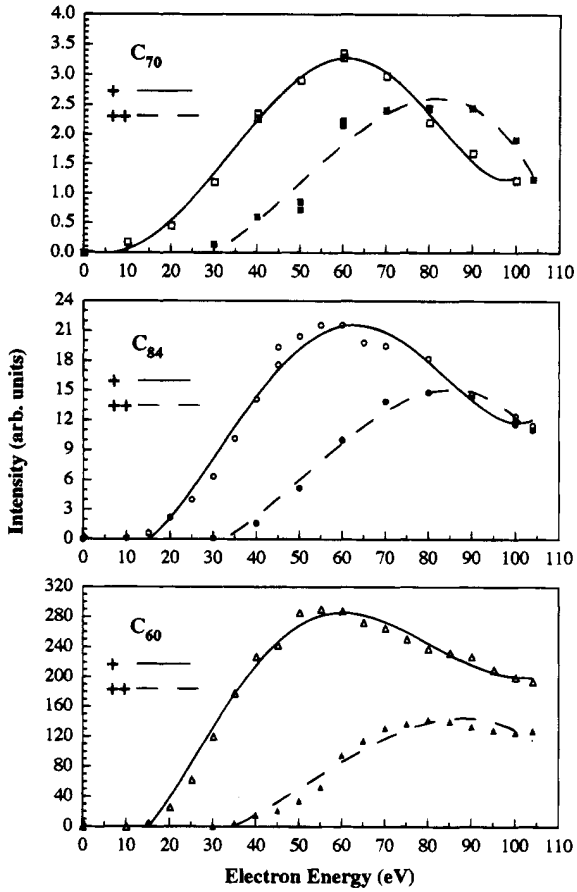

Figure 2. Variation of the intensity of singly and doubly charged ions with electron-impact energy for (a) C_{70} (present work), (b) C_{84} (present work), and (c) C_{60} (ref 5).

For the C_{84}-rich mixture, the signals of various mass species were monitored as the source temperature was varied from 800 to 950 K to obtain data on vaporization properties of such species. Next, the specimen was annealed for 2 h at 950 K to eliminate all mass peaks with the exception of those resulting from C_{84} and C_{70} (the resulting mixture of C_{70} and C_{84} will be referred to as the "mixture"). The intensities of various electron-impact-ionization products of these mixture clusters were monitored as electron energy was varied from 0 to 104 eV.

The scattering experiments of C_{84} from the mixture were carried out by varying the target temperature from 550 to 1200 K. For scattering experiments with C_{70}, the commercially available, pure specimen was put in the source tube after the C_{84} measurements were completed.

Results and Discussion

Electron-Impact-Ionization Efficiency. The main ionized species formed by electron-impact ionization of C_{60}, C_{70}, and C_{84} were singly and doubly charged parent ions. Within the range of electron energy used, fragmentation of these species was below detection limits. Figure 2a,b shows the variation of the observed intensities of C_{70}^+, C_{70}^{2+}, C_{84}^+, and C_{84}^{2+} with electron energy. Figure 2c from ref 5 is shown here for comparison. The ionization behavior of various fullerenes is remarkably similar. The singly charged mass species all show a threshold for ionization at ~15 eV and a maximum at 60 eV, while the doubly charged species have a threshold for ionization of ~35 eV and a maximum at ~85 eV. However, it appears that doubly ionized species for C_{70} and C_{84} form a larger percentage of the total ionization than for C_{60}.

Vaporization Properties of Higher Fullerenes. Figures 3a–c shows the Arrhenius plots of the intensities of singly

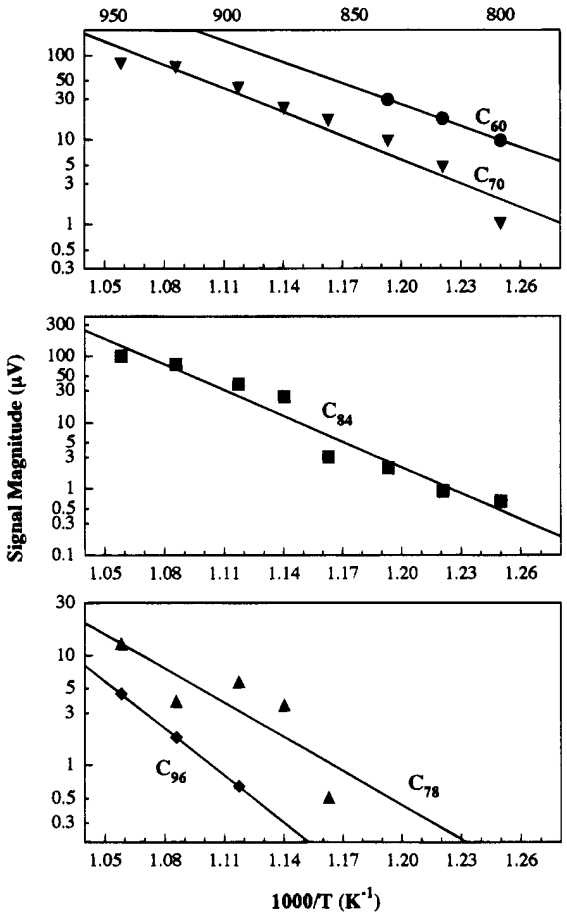

Figure 3. Knudsen cell source temperature dependence of the modulated mass spectrometer signal of various fullerenes in the mixture.

ionized C_{60}, C_{70}, C_{78}, C_{84}, and C_{96} at the QMS ionizer versus the reciprocal of the Knudsen cell temperature. The QMS is a density-sensitive detector, where density is given by the flux of molecules at the ionizer divided by the average velocity of the molecules. For constant flux the signal appears to decrease as the temperature of the Knudsen cell is raised because the average velocity is proportional to the square root of the temperature of the Knudsen cell. The results shown in Figure 3 are corrected for this factor. The slopes of the best-fit lines through each set of data points which represent the heat of sublimation of C_{60}, C_{70}, C_{78}, C_{84}, and C_{96} are 39 ± 5, 43 ± 5, 47 ± 18, 59 ± 6, and 65 ± 11 kcal/mol, respectively. The error values are 1σ determined from the least squares fitting. Since the mixture contained only a small percentage of C_{96}, only three data points were obtained. Therefore, the error for C_{96} was determined from the signal-to-noise ratio. Our results for C_{60} and C_{70} are in good agreement with Abrefah et's al.,[3] values of 38 ± 1 and 45 ± 1 kcal/mol and Pan et's al.,[2] values of 40 ± 1 and 43 ± 2 kcal/mol. Baba et al.[4] reported 43 ± 2 and 47 ± 2 kcal/mol for C_{60} and C_{70}. The heat of sublimation measured by Baba et al. for C_{60} is higher than that measured here or by Abrefah et al. or Pan et al.

We measured the same values for the heats of sublimation of C_{60} and C_{70} whether we used a pure sample or the higher fullerene mixture. This suggests the fullerene mixture is ideal. We are not aware of any prior measurements of heats of sublimation for C_{78}, C_{84}, and C_{96}. Baba et al.[17] reported the enthalpies of sublimation for mixtures of C_{60} and C_{70}. For mixtures containing 7−71 mol % C_{70} the enthalpies varied from 41.8 to 44.1 for C_{60} and 43.8 to 48 for C_{70}. The reported error for these measurements is 2 kcal/mol. Within the error limits of our measurements it is not possible to determine whether the mixture behaved as an ideal solution or not. However, from the results of Baba et al. above we can expect the deviation of values of the heat of sublimation for pure compounds not to exceed the error values in our measurements. We are pursuing work on improving extraction techniques in order to obtain pure specimens of higher fullerenes.

With time, the concentration of the trace fullerenes such as C_{60} was exhausted. First, the C_{60} signal started to reduce exponentially with time, while the Knudsen cell temperature remained constant at 850 K. Next, this trend was repeated with the exhaustion of C_{78} and C_{96} at 950 K. This method provided a desirable means of obtaining a source for the later experiments investigating the scattering of C_{84} from the silicon (100) surface.

We obtained an estimate of the partial pressure of the C_{84} from the known vapor pressures of C_{60} and C_{70} as follows: the mass spectrometer signal is proportional to the flux (and therefore to the vapor pressure in the Knudsen cell) by

$$S = k\sigma t\gamma\frac{P}{T} \tag{1}$$

where σ is the ionization cross section, t is the transmission efficiency, γ is the secondary electron multiplier coefficient, P is the partial pressure, T is the temperature of the gas in the Knudsen cell, and k is a geometric factor. From eq 1, the ratio of the signals of C_{60} and C_{70} at the same temperature is

$$\frac{S_{70}}{S_{60}} = \frac{\sigma_{70}}{\sigma_{60}}\frac{t_{70}}{t_{60}}\frac{\gamma_{70}}{\gamma_{60}}\frac{P_{70}}{P_{60}} \tag{2}$$

Since the postacceleration method is used for the electron multiplier first dynode (i.e. conversion dynode technique), γ should be about the same for both C_{60} and C_{70}. We had previously measured the vapor pressures of C_{60} and C_{70} by the microbalance technique as a function of temperature (2).

$$P_{60} = 3.0 \times 10^{7} \exp\left[\frac{-38\ \text{kcal/mol}}{RT}\right] \text{Torr}$$

$$P_{70} = 1.0 \times 10^{9} \exp\left[\frac{-45\ \text{kcal/mol}}{RT}\right] \text{Torr} \tag{3}$$

where R is the gas constant. With eqs 2 and 3 and Figure 3 we obtain the following ratio:

$$\frac{\sigma_{70}}{\sigma_{60}}\frac{\gamma_{70}}{\gamma_{60}}\frac{t_{70}}{t_{60}} = 0.35 \tag{4}$$

The addition of 10 carbons to the cage results in the reduction of the QMS factor ($\sigma\gamma t$) by a factor of ~3. Assuming the same trend to hold for C_{84} with respect to C_{70}, we may obtain the following estimate of the vapor pressure of C_{84}:

$$P_{84} = 7.0 \times 10^{12} \exp\left[\frac{-59\ \text{kcal/mol}}{RT}\right] \text{Torr} \tag{5}$$

The dependence of the heat of sublimation on the fullerene mass is plotted in Figure 4. The solid line represents the values proposed by Ruoff[18] using first-order molecular connectivity theory and the empirical coefficients from a linear fit to results obtained from polycyclic aromatic hydrocarbons (PAHs). The rather good agreement between our results and the extrapolation of the results for PAHs is remarkable considering the three-dimensional nature of the fullerene molecules.

High-Temperature Reaction of Fullerenes with Silicon. Moalem et al.[5] investigated the scattering of C_{60} from SiO_2 as a function of temperature. The interaction was shown to consist

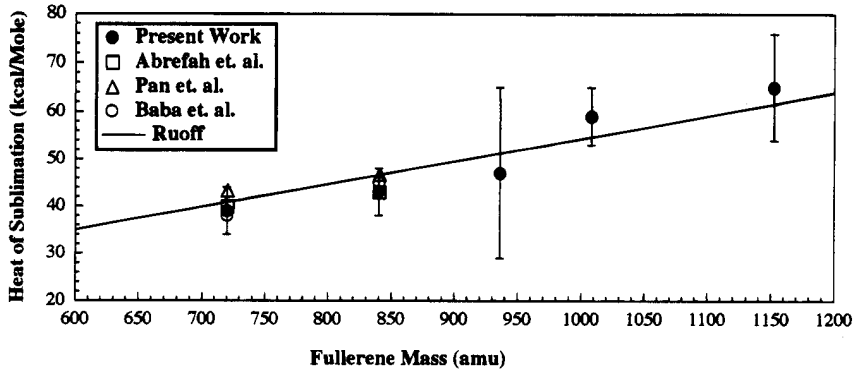

Figure 4. Dependence of the heat of sublimation of fullerenes on the mass of the cluster. The solid line is for the model by Ruoff.[18]

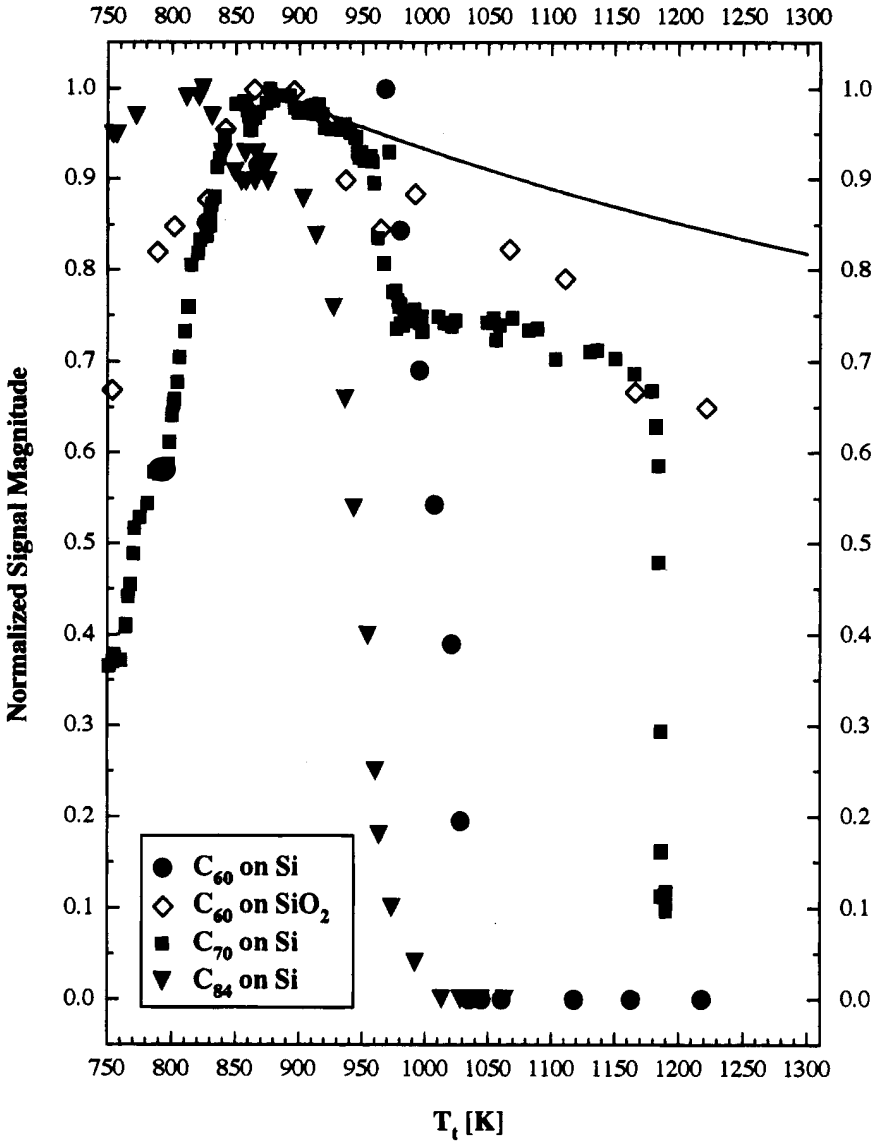

Figure 5. Scattered signal of fullerenes from Si and SiO_2 as a function of temperature. The C_{60} data on SiO_2 are taken from ref 4, and the C_{60} data on Si are taken from ref 1. The solid line is the expected decline of the signal due only to thermal accommodation to the surface temperature.

of surface adsorption with near perfect sticking probability, followed by the radial surface diffusion out of the beam spot and thermal desorption. At high temperatures (i.e. >850 K), the desorption rate is large, and therefore, the residence time of C_{60} on the surface and, correspondingly, the surface diffusion are negligibly small. In this regime, the only effect of the adsorption–desorption process is the thermal accommodation of the scattering species to the target temperature with a thermal accommodation coefficient, α_{th}, near unity. The density-sensitive signal of QMS correspondingly shows a reduction of the observed signal with the inverse of the square root of the target temperature. The net result of diffusion dominance at low temperature and thermal accommodation at high temperature is the observation of a signal peak at 880 K.

Figure 5 shows a comparison of the observed signals of scattered C_{60},[1] C_{70}, and C_{84} from Si with that of C_{60} from SiO_2.[5] Each signal is normalized with respect to its maximum value. The open circles represent the signal of C_{60} scattering from SiO_2,

and the solid line represents that of the expected signal for α_{th} equal to unity. At very high surface temperatures the C_{60} molecule fragments to C_{58} and adsorbed carbon on SiO_2.[19] This process can dissociate up to 5% of the incident C_{60} molecules at 1100 K. Thus, the open diamonds deviate from perfect accommodation to lower values. Up to surface temperatures of 1200 K, the fragmentation of the C_{60} on SiO_2 is small as compared to the reduction of the scattered signal for C_{60}, C_{70}, and C_{84} from silicon (see below).

The scattering of fullerenes from silicon is profoundly different from that from SiO_2. All fullerenes undergo a reaction with silicon to the extent that above 1200 K no fullerenes (or any other carbon-bearing species) desorb from the surface. We have investigated the reaction of C_{60} with silicon in detail previously.[1] The analysis of the surface showed the complete breakdown of the C_{60} cage accompanied with the growth of an epitaxial silicon carbide film on the surface. The growth rate of this SiC film was limited only by the arrival rate of C_{60} from the source and the arrival rate of Si by the diffusion through the SiC layer. The reaction of C_{60} with Si proceeds at temperatures above 970 K. By contrast, the C_{84} reaction with silicon starts at 820 K, substantially lower than C_{60}. Since the reduction in the scattered C_{84} and C_{60} signal depends on the flux of Si to the reacting surface by diffusion and the flux of C_{84} is much less than the flux of C_{60}, the temperature at which the scattered signal declines may only be indicative of the rate of silicon arrival and not the fragmentation probability. C_{60} begins to fragment on silicon at 900 K.[20] Thus, the onset of decline at 820 K for C_{84} suggests that the C_{84} may be slightly less stable than C_{60} on silicon. The 80 K lower temperature for C_{84} fragmentation may be significant for commercial production of SiC films for microelectronics applications, where attaining the lowest processing temperatures for the wafers is essential.

The reaction of C_{70} with silicon proceeds above 940 K. The decline in the scattered C_{70} signal from 850 to 940 K is due to thermal accommodation. At this point the signal abruptly drops by 20% of its maximum value to a plateau by 980 K. In the plateau area from 980 to 1180 K, the scattered signal again declines only due to thermal accommodation. This peculiar behavior may be related to the geometric structure of the C_{70} molecule as compared to C_{60} and C_{84} nanoclusters. It is plausible that the sticking probability or reaction of the "rugby-ball"-shaped C_{70} nanocluster may depend on the orientation at which it impinges on the surface; the C_{60} structure and the D_2 and D_{2d} isomers of C_{84} are essentially spherical.

Low-Temperature Scattering of Fullerenes from Si Surface. At low temperatures ($T < 850$ K) where surface diffusion is significant, the scattering of fullerenes from solid surfaces can be used to investigate the desorption rate and diffusivity of the fullerenes. Figure 6 shows the temperature dependence of the unmodulated normalized signals of C_{70} and C_{84} scattered from silicon. The signals have been converted from density to flux-sensitive detection.

At low temperatures between 750 and 570 K, reduction of the desorption rate of fullerenes from the sample and the increase in the long-range surface diffusion of fullerenes from the beam spot (3 mm in diameter) to the edge of the surface (6 mm in diameter) cause a decrease of the observed signal. The molecules that reach the edge of the target desorb into a solid angle out of the QMS field of view. As the temperature of the target is raised, the desorption rate of fullerenes increases, and as a result, a smaller fraction of the fullerenes succeed at diffusing to the specimen edge.

From Figure 6, the C_{70} signal saturates at 630 K, while the C_{84} signal does not saturate until 850 K. We model the process

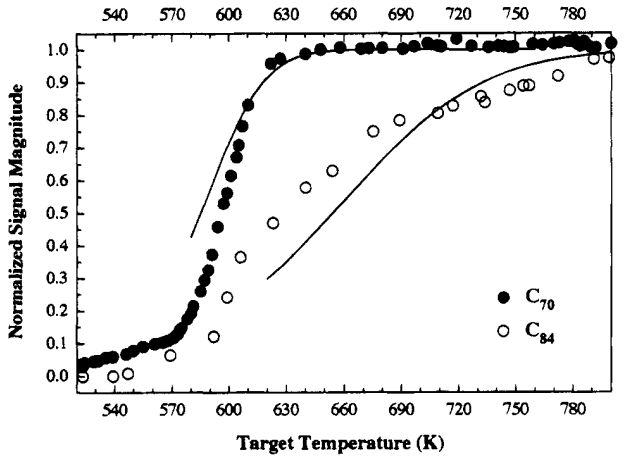

Figure 6. Unmodulated scattered signal of C_{70} and C_{84} from Si as a function of temperature. The solid lines are fit to the model presented in the text for C_{70} and C_{84}.

as steady-state diffusion and desorption with a spatially dependent source term. The mass balance equation for the fullerenes on the surface may be written as

$$D_s\frac{1}{r}\frac{d}{dr}\left(r\frac{dC}{dr}\right) - k_dC + \eta_sI_0f(r) = 0 \tag{6}$$

where $C(r)$ is the surface concentration, D_s is the surface diffusivity, and k_d is the desorption rate constant of the fullerenes. The sticking probability, η_s, is unity: I_0 is the flux of the incident fullerenes on the surface; and $f(r)$ is the radial profile of the incident beam. For this problem, $f(r)$ is

$$f(r) = \begin{cases} 1; & 0 \le r \le R_b \\ 0; & R_b < r \le R_0 \end{cases} \tag{7}$$

where R_b (=1.5 mm) is the radius of the beam spot and R_0 (=3 mm) is the radius of the specimen. Boundary conditions are

$$\frac{dC}{dr}(r=0) = 0 \qquad C(r=R_0) = 0 \tag{8}$$

The observed normalized signal is given by

$$S(T) = 1 + \frac{2\pi RD_s\left[\frac{dC}{dr}(r=R_0)\right]}{\eta I_0(\pi R_b^2)} \tag{9}$$

The equation can be normalized by the following choice of the variables and parameters,

$$\theta = \frac{D_SC}{\eta_sI_0R_0^2};\ \eta = \frac{r}{R_0};\ m = \frac{k_dR_0^2}{D_s} \tag{10}$$

$$\frac{d^2\theta}{d\eta^2} + \frac{1}{\eta}\frac{d\theta}{d\eta} - m\theta + f(\eta) = 0 \tag{11}$$

$$f(\eta) = \begin{cases} 1; & 0 \le \eta \le \dfrac{R_b}{R_0} \\ 0; & \dfrac{R_b}{R_0} < \eta \le 1 \end{cases} \tag{12}$$

$$\frac{d\theta}{d\eta}(\eta=0) = 0;\ \theta(\eta=1) = 0 \tag{13}$$

and the expression for the normalized signal S is

$$S = 1 + 2\left(\frac{R^2}{R_b^2}\right)\left[\frac{d\theta}{d\eta}(\eta=1)\right] \quad (14)$$

For a temperature dependence of m,

$$m = m_0 \exp\left(-\frac{Q_m}{RT}\right) \quad (15)$$

the dependence of S on T can be obtained numerically.

The solid lines in Figure 6 represent the best fits for C_{70} and C_{84} data. The values of the parameter m are as follows:

$$m_{70} = 2.5 \times 10^{15} \exp\left[\frac{-40 \text{ kcal/mol}}{RT}\right]$$
$$m_{84} = 7.0 \times 10^{7} \exp\left[\frac{-22 \text{ kcal/mol}}{RT}\right] \quad (16)$$

The ratio of desorption rate constant to diffusion coefficient can be obtained by dividing m by the square of the sample radius, R_0. As expected, m_{70} is much larger than m_{84}, indicating that for C_{84} surface diffusivity is significantly more important than desorption as compared to C_{70}. At 650 K, m_{70} is a factor of 36 larger than m_{84}. m_{84} is smaller than m_{70} because either the desorption rate constant, k_d, is smaller or the diffusion coefficient is larger, or both. The k_d for C_{84} should be smaller than k_d for C_{70} by analogy to the heat of sublimation results above. If k_d was independently determined by other techniques such as temperature-programmed desorption, the diffusion coefficients for C_{84} and C_{70} could be extracted.

Conclusions

We measured the electron-impact-ionization efficiency of C_{60}, C_{70}, and C_{84} over the range 0−104 eV in electron energy and the heat of sublimation of the fullerenes from 800 to 950 K. The singly charged mass species all show a threshold for ionization at ~15 eV and a maximum at 60 eV, while the doubly charged species have a threshold for ionization of ~35 eV and a maximum at ~85 eV. The heats of sublimation of C_{60}, C_{70}, C_{78}, C_{84}, and C_{96} were measured to be 39 ± 5, 43 ± 5, 47 ± 18, 59 ± 6, and 65 ± 11 kcal/mol, respectively. The values for C_{60} and C_{70} agree well with prior investigations. The vapor pressure of C_{84} was estimated to be $P_{84} = 7.0 \times 10^{12} \exp[-59$ kcal/mol/RT] Torr.

Interactions of C_{70} and C_{84} with a clean silicon surface were investigated. The reaction threshold temperatures for C_{70} and C_{84} are 940 and 820 K, respectively. The behavior of C_{70} is surprisingly different from both C_{60} and C_{84}. Twenty percent of the incident C_{70} decomposes at ~1000 K, and the remaining 80% does not decompose until a target temperature of ~1200 K is reached. From the low-temperature data, the ratio of desorption rate constant to diffusion coefficient for C_{70} and C_{84} was calculated to be $2.7 \times 10^{16} \exp(-40$ (kcal/mol)/RT) and $7.8 \times 10^{7} \exp(-22$ (kcal/mol)/RT) cm^{-2}, respectively.

Acknowledgment. This work was supported by the U.S. Department of Energy, at Lawrence Livermore National Laboratory, under Contract No. W-7405-Eng-48. We appreciate Lorenza Moro and Chris Becker for acquiring the SALI spectrum. R.S.R. acknowledges *partial* support for the separation of higher fullerenes from soot from the "Advanced Chemical Processing Technology", which is consigned to the Advanced Chemical Processing Technology Research Association from the New Energy and Industrial Technology Development Organization and carried out under the Large-Scale Project administered by the Agency of Industrial Science and Technology, the Ministry of International Trade and Industry, Japan.

References and Notes

(1) Hamza, A. V.; Balooch, M.; Moalem, M. *Surf. Sci.* **1994**, *317*, L1129.
(2) Pan, C.; Sampson, M. P.; Chai, Y.; Hauge, R. H.; Margrave, J. L. *J. Phys. Chem.* **1991**, *95*, 2994.
(3) Abrefah, J.; Olander, D. R.; Balooch, M.; Siekhaus, W. J. *Appl. Phys. Lett.* **1992**, *60*, 1313.
(4) Baba, M. S.; Narasimhan, T. S. L.; Balasubramanian, R.; Sivaraman, N.; Mathews, C. K. *J. Phys. Chem.* **1994**, *98*, 1333.
(5) Moalem, M.; Balooch, M.; Hamza, A. V.; Siekhaus, W. J.; Olander, D. R. *J. Chem. Phys.* **1993**, *99*, 4855.
(6) Ettl, R.; Chao, I.; Diederich, F.; Whetten, R. L. *Nature* **1991**, *353*, 149.
(7) Diederich, F.; Whetten, R. L.; Thilgen, C.; Ettl, R.; Chao, I.; Alvarez, M. M. *Science* **1991**, *254*, 1768.
(8) Raghavachari, K. *Chem. Phys. Lett.* **1992**, *190*, 397.
(9) Bakowies, D.; Kolb, M.; Thiel, W.; Richard, S.; Ahlrichs, R.; Kappes, M. M. *Chem. Phys. Lett.* **1992**, *200*, 411.
(10) Wang, X.-D.; Wang, T.; Hashizume, H.; Shinohara, H.; Saito, Y.; Nishina, Y.; Sakurai, T. *Phys. Rev.* **1993**, *B47*, 15923.
(11) Saito, Y.; YoshiKawa, T.; Fujimoto, N.; Shinohara, H. *Phys. Rev.* **1993**, *B48*, 9182.
(12) Poirier, D. M.; Weaver, J. H.; Kikuchi, K.; Achiba, Y. *Z. Phys.* **1993**, *D26*, 79.
(13) Armbruster, J. F.; Roth, M.; Romberg, H. A.; Sing, M.; Schmidt, M.; Schweiss, P.; Adelmann, P.; Golden, M. S.; Fink, J.; Michel, R. H.; Rockenberger, J.; Hennrich, F.; Kappes, M. M. *Phys. Rev.* **1994**, *B50*, 4933.
(14) Armbruster, J. F.; Romberg, H. A.; Schweiss, P.; Adelmann, P.; Knupfer, M.; Fink, J.; Michel, R. H.; Rockenberger, J.; Hennrich, F.; Kappes, M. M. *Z. Phys.* **1994**, *B95*, 469.
(15) Hino, S.; Matsumoto, K.; Hasegawa, S.; Inokuchi, H.; Morikawa, T.; Takahashi, T.; Seki, K.; Kikuchi, S.; Suzuki, S.; Ikemoto, I.; Achiba, Y. *Chem. Phys. Lett.* **1992**, *197*, 38.
(16) Cheng, H.-P.; Whetten, R. L. *Chem. Phys. Lett.* **1992**, *197*, 44.
(17) Baba, M. S.; L. Narasimhan, T. S.; Balasubramian, R.; Sivaraman, N.; Mathews, C. K. *J. Phys. Chem.* **1994**, *98*, 1333.
(18) Ruoff, R. S. *Chem. Phys. Lett.* **1993**, *208*, 256.
(19) Hamza, A. V.; Balooch, M.; Moalem, M.; Olander, D. R. *Chem. Phys. Lett.* **1994**, *228*, 117.
(20) Balooch, M.; Hamza, A. V. *Appl. Phys. Lett.* **1993**, *63*, 150.

JP951641X